Multi-bounce resonances in the interaction of walking droplets

George Zhang [*], Ivan C. Christov [†‡], Aminur Rahman[*§]

Abstract

Discrete dynamical models of walking droplets ("walkers") have allowed swift numerical experiments revealing heretofore unobserved quantum statistics and related behaviors in a classical hydrodynamic system. One such model shows evidence of the empirically elusive n-bounce resonance and chaotic scattering in solitary-wave interactions investigated using covariant nonlinear field theory with polynomial self-interaction. We present experimentally testable predictions of n-bounce resonances between walkers. An exhaustive numerical investigation of the model reveals the usual fractal structure of resonances in the velocity in–velocity out diagram for colliding walkers. We suggest some avenues for further theoretical analysis of walker collisions, which may connect this discrete model back to the field-theoretic setting.

1 Introduction

From afar it may seem like droplets "walking" on a vibrating fluid bath and solitary-wave solutions to nonlinear wave equations have little in common. Unlike solitary waves, waves surfacing in the fluid bath, and sustaining the walking droplet, are hardly localized disturbances, nor do they maintain their shape. (Though solitary waves exist on shallow water in a different context [27, 18, 9].) With each impact between the droplet and its bath, a new eigenmode is excited in the surface wavefield. Further, a droplet drives the wave generation and propagation whereas, after an initial perturbation, a solitary wave is self-sustained and does not require external energy input to continue propagating—its dynamics being set by the balance of nonlinearity and dispersion in the medium. However, we find that, qualitatively, the dynamics of colliding and interacting walking droplets ("walkers") are reminiscent of the collisions and interactions of solitary waves [7, 12] under a generic covariant nonlinear field theory, such as the so-called ϕ^4 one arising in many branches of physics [20, 34].

[*]Department of Applied Mathematics, University of Washington
[†]School of Mechanical Engineering, Purdue University
[‡]Department of Computer Science, University of Nicosia
[§]Corresponding arahman2@uw.edu

This paper is dedicated to the memory of our friend, mentor, and colleague, Denis Blackmore. Skål, 🍸

One of the remarkable aspects of the walker phenomenon is the wave-like statistics arising from the horizontal motion of the droplet, which has been well-delineated in reviews by Bush [3, 5, 4], Bush and Oza [6], and Rahman and Blackmore [25]. However, most of the wave-like statistics in both experiments [17, 28, 24] and dynamical models [11, 24, 10] have been shown for a single droplet. One interesting deviation from this comes in the form of a string of droplets exhibiting a traveling wave [32, 31]. Between a score or two of droplets are placed around an annulus. As the vertical acceleration of the bath vibration is increased, the droplets start to destabilize, and eventually, a circumferential perturbation from the initial position is transferred through neighboring droplets and continues around the annulus. In this communication, we show the existence of solitary wave-like statistics in a discrete dynamical model of the mutual interaction of two walking droplets, as shown in Fig. 1.

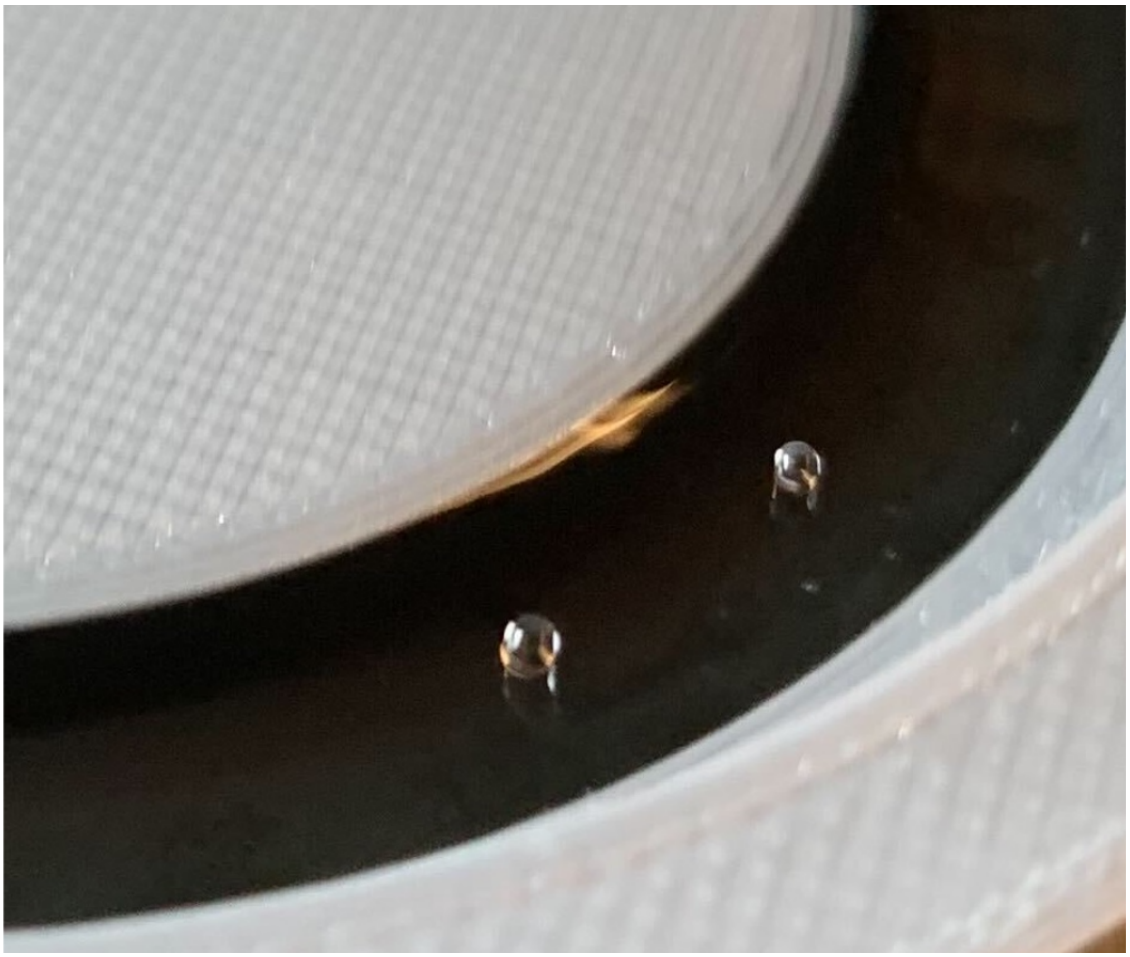

Figure 1: A picture of two walking droplets on an annulus interacting with each other through the waves they produce on the fluid bath's surface.

Covariant nonlinear field theories with polynomial self-interaction arise in a number of fields from condensed matter physics [33] to materials science [16] to high-energy physics and cosmology [26, 34], see also the overview by [29]. In the simplest one-dimensional context, these theories take the form of a wave equation (d'Alembertian) forced by a nonlinear (poly-

nomial) function of the dependent variable. These nonlinear wave equations (also referred to as nonlinear Klein–Gordon equations, by a loose analogy to the Klein–Gordon equation arising in quantum field theory) exhibit self-sustained, localized (solitary) traveling wave solutions (so-called topological solitons [20] or domain walls [33]). These solitary waves can interact, by for example being sent on a collision course with each other. Perhaps not unexpectedly, the interactions are complex: the solitary waves may repel each other, they may undergo a successive series of collisions ("bounces") as if they are unable to escape each others' pull, or they may form a permanent bound state [8, 1, 2]. It is hypothesized that these behaviors may be simple models of subatomic particle interactions [21]. However, the study of collisions of solitary waves in nonlinear field theories remains phenomenological, without direct experimental confirmation (see, e.g., the discussion in [15]). In this communication, we show that a strikingly similar collision phenomenology is also observed in the classical system of two walking droplets interacting with each other.

To this end, we consider a simplified dynamical model of the walker interactions derived in the sequel. Then in Sec. 3 we present observations of solitary wave-like behavior similar to n-bounce resonance exhibited by the interacting droplets. Finally, we conclude with a discussion of the connections with solitons and future work to produce physical realizations of the observed effect.

2 The discrete dynamical model

In this section we model the self-propulsion and interaction between the droplets as a discrete dynamical system. We start with Eq. (23) of [23]:

$$v_i(n+1) = C\Bigg[v_i(n) + K\sin\big(\omega v_i(n)\big)e^{-\nu v_i(n)^2} + K\eta(\gamma n)\sum_{m=1,\,m\neq i}^{M}\operatorname{sgn}\big(x_i(n)-x_m(n)\big)e^{-\nu[x_i(n)-x_m(n)]^2}\Bigg], \quad (1)$$

where $v_i(n)$ and $x_i(n)$ are the velocity and the position, respectively, of the i^{th} droplet (walker) after their n^{th} impact with the surface of the fluid reservoir below them, including the mutual effects of up to M other walkers. The 'bump function' η is defined as

$$\eta(\xi) = \begin{cases} \exp\left(1-\frac{1}{1-\xi^2}\right), & \xi\in(-1,1),\\ 0, & \xi\notin(-1,1). \end{cases} \quad (2)$$

Further, $\gamma\in[0,1]$ and $\nu\in\mathbb{R}^+$ are damping factors, while K and C are parameters modeling the effect of 'kicks' on the droplets (walkers).

Equation (1) is supplemented by the kinematic relation

$$x_i(n+1) = x_i(n) + v_i(n+1), \quad (3)$$

which advances the walker position after the n^{th} bounce.

In [23], a set of interacting droplets converged to a state in which they are equispaced around the circle. In this study, we wish to model the interaction of two droplets propelled towards each other with equal and opposite velocities: $v_1(0) = v_{\text{in}}$ and $v_2(0) = -v_{\text{in}}$. We know empirically that the droplets repel each other through their respective wavefields, and the strength of the repulsion increases as the droplets get closer to each other. Therefore, we simplify Eq. (1) as

$$v_i(n+1) = C\Big[v_i(n) + K\sin\big(\omega v_i(n)\big)e^{-\nu v_i(n)^2} + K\eta\big(x_i(n) - x_m(n)\big)\,\mathrm{sgn}\,\big(x_i(n) - x_m(n)\big)e^{-\nu[x_i(n)-x_m(n)]^2}\Big] \quad (4)$$

for the two-droplet system in the present work. An example of the type of behavior produced by the model is shown in Fig. 2.

In this figure, two droplets are starting from effective infinity (Fig. 2(a)), $-x_1(0) = x_2(0) = 1$; i.e., the boundary of the support in (2). From these initial points, the droplets are given an initial velocity of $v_1(0) = -v_2(0) = v_{\text{in}}$. The droplets approach each other until the repulsion from their interaction overcomes their own inertia, after which they reverse direction (Fig. 2(b)). This is known as a *bounce*. The droplets can bounce once, several times, or be bound forever. If the droplets are not in a bound state, they eventually escape and go beyond effective infinity (Fig. 2(d)). In this figure, a two-bounce scattering is shown where the droplets move away from each other, but then approach one another again ((Fig. 2(c))). In Fig. 2(e) we present the complete iterated trajectory of the droplet for the two-bounce case with the relevant events from Fig. 2(a-d) labeled on the plot.

3 Collision phenomenology and multi-bounce windows

In this section, we shall demonstrate the droplet interactions as modeled by (4). Throughout the section we will use $\omega = 31/2$, $\nu = \omega^2/8.4\pi^2$, and $K = -\pi e^{\nu\pi^2}/\sin(\pi\omega)$ [23]. We may also vary C to produce varying complexity in the velocity iterate space. For this section we $C = 1/5K$, which strikes a balance between the strength of the interaction and self-propulsion.

To demonstrate the existence of multi-bounce windows in the collision of $M = 2$ walkers, consider (4) with varying initial velocities. In Fig. 3 we present four illustrative cases for the behavior of the model. We first take an initial velocity of $v_{\text{in}} = 0.15$. The droplets approach each other and are then repelled with a strong enough force to escape past the support of (2) as shown in Fig. 3(a). We use $v_{\text{in}} = 0.01$ to produce the two-bounce scattering in Fig. 3(b), which is similar to the one shown in the schematic in Fig. 2. We may also get several bounces before escape as observed in Fig. 3(c), which uses an initial velocity of $v_{\text{in}} = 0.1335045$. Finally, we have a bound state in Fig. 3(d), where the droplets never escape. This is produced using $v_{\text{in}} = 0.135$.

Constructing a typical velocity in–velocity out diagram colored by the number of bounces the walkers perform seems to exhibit a fractal structure of windows as is the case in kink–anti-kink interactions of the ϕ^4 nonlinear field theory [13, 12]. As shown in Fig. 4(a), we have

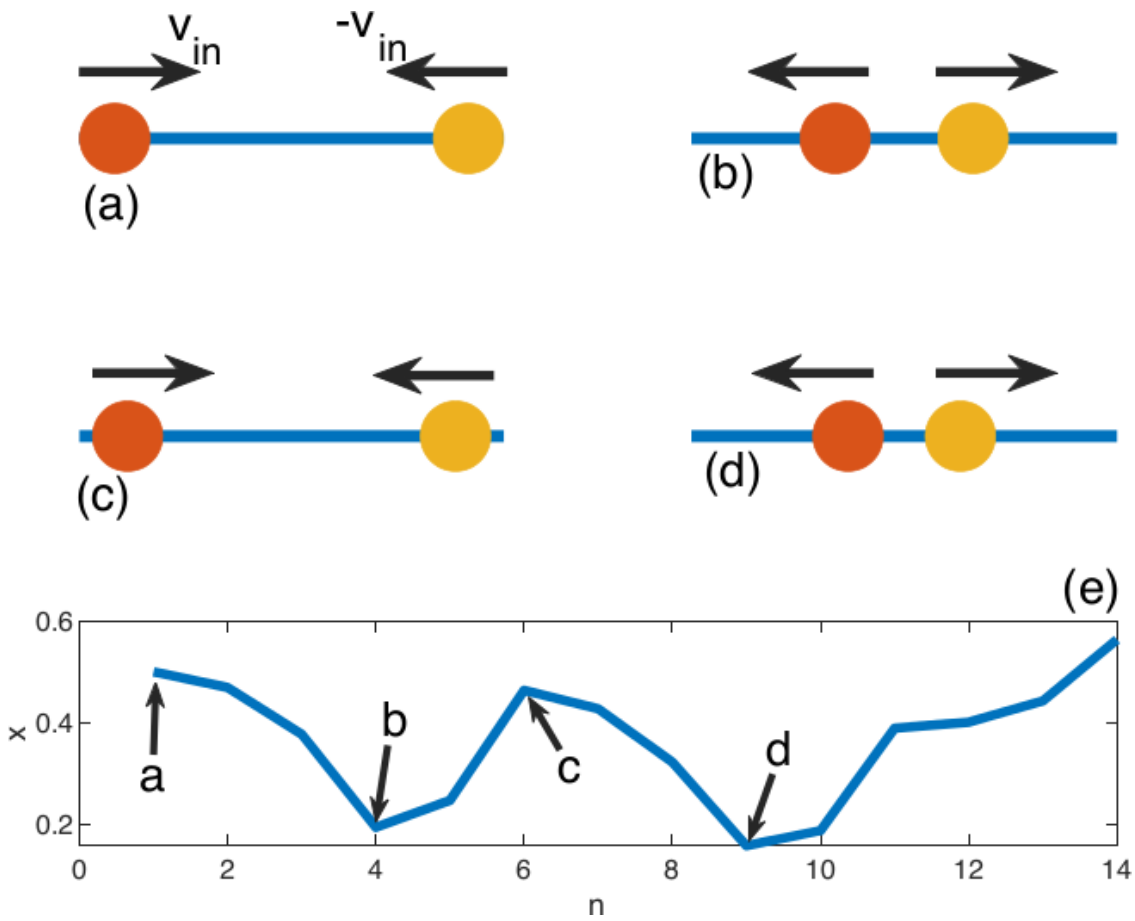

Figure 2: (a-d) Schematic of a pair of walkers undergoing a two-bounce scattering. The walkers approach each other from an initial position at effective infinity with an initial velocity (a), then they are repelled by their interaction (b), however, their interaction coupled with their self-propulsion (c) bring them back together (d), until they eventually escape each other's domain of influence. (e) The time-discrete trajectory of the left walker, with the events (a-d) labeled on it.

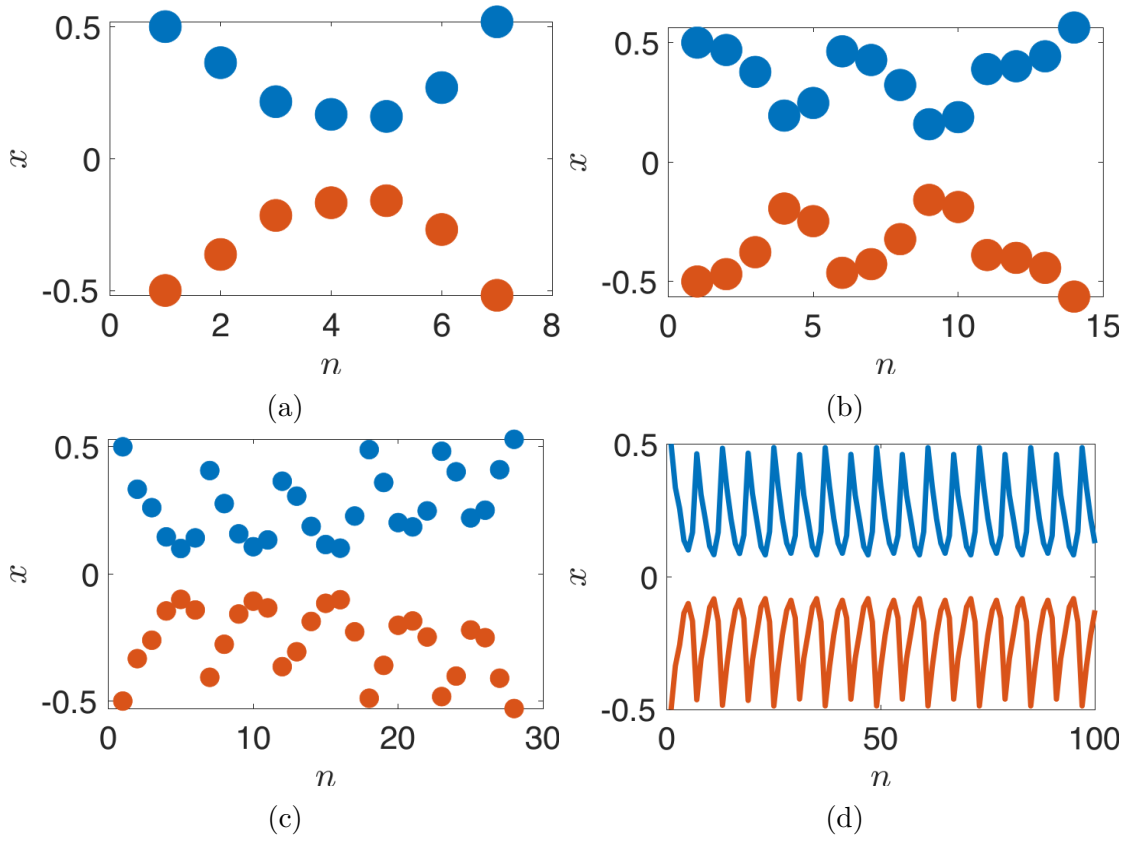

Figure 3: Example discrete walker trajectories exhibiting (a) a one-bounce with $v_{\text{in}} = 0.15$, (b,c) multi-bounce behavior with $v_{\text{in}} = 0.01$ and $v_{\text{in}} = 0.1335045$, respectively, and (d) a bound state with $v_{\text{in}} = 0.135$. For each plot we use the standard parameters $\omega = 31/2$, $\nu = \omega^2/8.4\pi^2$, and $K = -\pi e^{\nu\pi^2}/\sin(\pi\omega)$ [23], and $C = 1/5K$.

quite a range of relationships between the initial velocity v_{in} and the velocity with which it escapes v_{out}. Sometimes it produces iterates that are seemingly chaotic, and at other times it produces an orderly continuous curve. This is reminiscent of iterate space produced by map models of the solitary wave interactions [13, 12], which have also been observed to be seemingly chaotic. Since this produces a fractal structure, it is natural to compute the fractal dimension. We use the Minkowski–Bouligand dimension,

$$d = \lim_{\varepsilon \to 0} \frac{\ln(N(\varepsilon))}{\ln(1/\varepsilon)}, \tag{5}$$

with the progression of the number of box coverings, $N(\varepsilon)$ for respective length, ε, of the square covering shown in Fig. 4(b). Using this definition gives us a dimension of $d \approx 0.95$. Details for how the dimension was calculated are given in Appendix A.3.

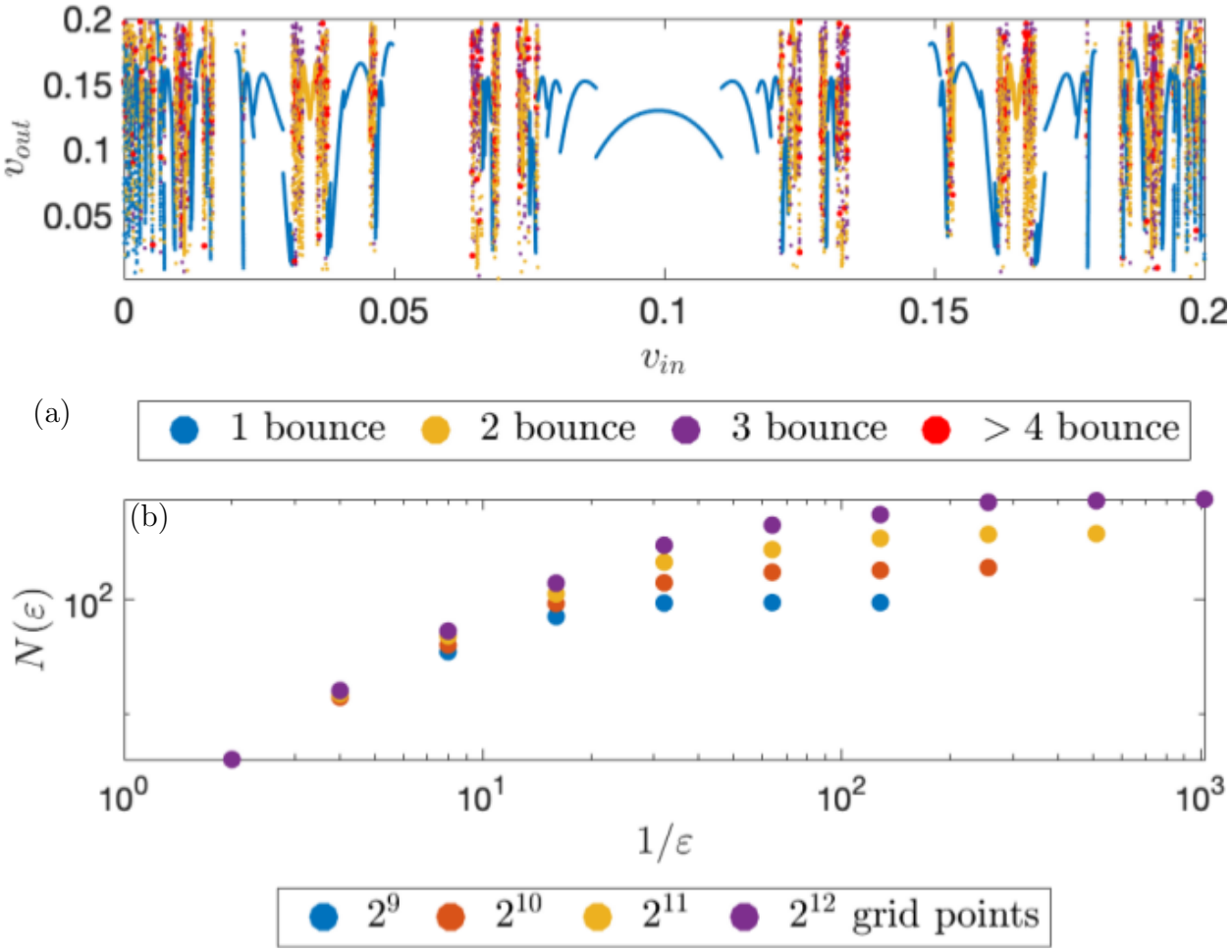

Figure 4: (a) Bounce windows with fractal structure. The markers are color-coded based on the number of bounces the droplets experienced before escaping. Blue represents one bounce, yellow represents two bounces, purple represents three bounces, and red represents four or more bounces. (b) Progression of the number of box coverings required to cover the entire plot (a) to illustrate the calculation of the Minkowski–Bouligand dimension.

4 Conclusion

In this communication we develop a phenomenological model modified from that of [23]. In Sec. 3 we observe that (4) exhibits single and multi-bounce behavior and bound states, which are often present in nonlinear solitary wave interactions. Further still, we observe fractal structure in the $v_{\text{in}} - v_{\text{out}}$ plot and compute the Minkowski–Bouligand dimension (5). All of these features are reminiscent of kink-antikink solitary wave interactions [14, 13, 1], which leads the way for promising future work.

It would certainly be presumptuous to claim that simulations from a reduced discrete dynamical model indicate that the physical system exhibits n-bounce resonance. However, we hope that this investigation may act as a compass for researchers to search for n-bounce resonances in the novel physical context of walking droplets and the corresponding experiments, drawing further analogies between concepts in nonlinear field theory and dynamics realizable in a bench-top experiment.

Acknowledgement

G.Z. and A.R. appreciate the support of the Department of Applied Mathematics at the University of Washington. I.C.C. would like to acknowledge the hospitality of the University of Nicosia, Cyprus, where this work was completed thanks to a Fulbright U.S. Scholar award from the U.S. Department of State.

References

[1] Anninos, P., Oliveira, S., Matzner, R.A., 1991. Fractal structure in the scalar $\lambda(\varphi^2 - 1)^2$ theory. Phys. Rev. D 44, 1147–1160. doi:10.1103/PhysRevD.44.1147.

[2] Belova, T.I., Kudryavtsev, A.E., 1997. Solitons and their interactions in classical field theory. Phys. Usp. 40, 359–386. doi:10.1070/PU1997v040n04ABEH000227.

[3] Bush, J.W.M., 2010. Quantum mechanics writ large. Proc. Natl Acad. Sci. USA 107, 17455–17456. doi:10.1073/pnas.1012399107.

[4] Bush, J.W.M., 2015a. The new wave of pilot-wave theory. Phys. Today 68, 47–53. doi:10.1063/PT.3.2882.

[5] Bush, J.W.M., 2015b. Pilot-wave hydrodynamics. Annu. Rev. Fluid Mech. 47, 269–292. doi:10.1146/annurev-fluid-010814-014506.

[6] Bush, J.W.M., Oza, A.U., 2021. Hydrodynamic quantum analogs. Rep. Prog. Phys. 84, 017001. doi:10.1088/1361-6633/abc22c.

[7] Campbell, D.K., 2019. Historical overview of the ϕ^4 model, in: Kevrekidis, P.G., Cuevas-Maraver, J. (Eds.), A Dynamical Perspective on the ϕ^4 Model: Past, Present and Future". Springer International Publishing, Cham, Switzerland. volume 26 of *Nonlinear Systems and Complexity*. chapter 1, pp. 1–22. doi:10.1007/978-3-030-11839-6_1.

[8] Campbell, D.K., Schonfeld, J.F., Wingate, C.A., 1983. Resonance structure in kink-antikink interactions in ϕ^4 theory. Physica D 9, 1–32. doi:10.1016/0167-2789(83)90289-0.

[9] Dauxois, T., Peyrard, M., 2006. Physics of Solitons. Cambridge University Press, New York.

[10] Ferrandez Quinto, G., Rahman, A., 2023. Stochastic discrete dynamical model for the hydrodynamic analog of a quantum mirage. preprint doi:10.48550/arXiv.2302.00829.

[11] Gilet, T., 2016. Quantumlike statistics of deterministic wave-particle interactions in a circular cavity. Phys. Rev. E 93, 042202. doi:10.1103/PhysRevE.93.042202.

[12] Goodman, R.H., 2019. Mathematical analysis of fractal kink-antikink collisions in the ϕ^4 model, in: Kevrekidis, P.G., Cuevas-Maraver, J. (Eds.), A Dynamical Perspective on the ϕ^4 Model: Past, Present and Future". Springer International Publishing, Cham, Switzerland. volume 26 of *Nonlinear Systems and Complexity*. chapter 4, pp. 75–91. doi:10.1007/978-3-030-11839-6_4.

[13] Goodman, R.H., Haberman, R., 2005. Kink-antikink collisions in the ϕ^4 equation: The n-bounce resonance and the separatrix map. SIAM J. Appl. Dyn. Sys. 4, 1195–1228. doi:10.1137/050632981.

[14] Goodman, R.H., Haberman, R., 2007. Chaotic scattering and the n-bounce resonance in solitary-wave interactions. Phys. Rev. Lett 98, 104103. doi:10.1103/PhysRevLett.98.104103.

[15] Goodman, R.H., Rahman, A., Bellanich, M.J., Morrison, C.N., 2015. A mechanical analog of the two-bounce resonance of solitary waves: Modeling and experiment. Chaos 25, 043109. doi:10.1063/1.4917047.

[16] Gufan, Y.M., 1982. Structural Phase Transitions [in Russian]. Nauka, Moscow.

[17] Harris, D.M., Moukhtar, J., Fort, E., Couder, Y., Bush, J.W.M., 2013. Wavelike statistics from pilot-wave dynamics in a circular corral. Phys. Rev. E 88, 011001. doi:10.1103/PhysRevE.88.011001.

[18] Korteweg, D.J., de Vries, G., 1895. On the change of form of long waves advancing in a rectangular canal, and on a new type of long stationary waves. Phil. Mag. Ser. 5 39, 422–443. doi:10.1080/14786449508620739.

[19] Malomed, B.A., 2002. Variational methods in nonlinear fiber optics and related fields. Prog. Opt. 43, 71–193. doi:10.1016/S0079-6638(02)80026-9.

[20] Manton, N., Sutcliffe, P., 2004. Topological solitons. Cambridge University Press, New York. doi:10.1017/CBO9780511617034.

[21] Manton, N.S., 2008. Solitons as elementary particles: a paradigm scrutinized. Nonlinearity 21, T221. doi:10.1088/0951-7715/21/11/T01.

[22] Meiss, J.D., 1992. Symplectic maps, variational principles, and transport. Rev. Mod. Phys. 64, 795–848. doi:10.1103/RevModPhys.64.795.

[23] Rahman, A., 2018. Standard map-like models for single and multiple walkers in an annular cavity. Chaos 28, 096102. doi:10.1063/1.5033949.

[24] Rahman, A., 2023. Damped-driven system of bouncing droplets leading to deterministically diffusive behavior. preprint doi:10.48550/arXiv.2301.06041.

[25] Rahman, A., Blackmore, D., 2020. Walking droplets through the lens of dynamical systems. Mod. Phys. Lett. B 34, 2030009. doi:10.1142/S0217984920300094.

[26] Rajaraman, R., 1982. Solitons and Instantons. North Holland, Elsevier Science Publishers B.V., Amsterdam.

[27] Russell, J.S., 1845. Report on waves, in: Report of the fourteenth meeting of the British Association for the Advancement of Science. John Murray, London, pp. 311–390. URL: https://biodiversitylibrary.org/page/13141996.

[28] Sáenz, P.J., Cristea-Platon, T., Bush, J.W.M., 2018. Statistical projection effects in a hydrodynamic pilot-wave system. Nature Phys. 14, 315–319. doi:10.1038/s41567-017-0003-x.

[29] Saxena, A., Christov, I.C., Khare, A., 2019. Higher-order field theories: ϕ^6, ϕ^8 and beyond, in: Kevrekidis, P.G., Cuevas-Maraver, J. (Eds.), A Dynamical Perspective on the ϕ^4 Model. Springer Nature, Cham, Switzerland. volume 26 of *Nonlinear Systems and Complexity*. chapter 12, pp. 253–279. doi:10.1007/978-3-030-11839-6_12, arXiv:1806.06693.

[30] Sugiyama, T., 1979. Kink-antikink collisions in the two-dimensional ϕ^4 model. Prog. Theor. Phys. 61, 1550–1563. doi:10.1143/PTP.61.1550.

[31] Thomson, S.J., Couchman, M., Bush, J.W.M., 2020a. Collective vibrations of confined levitating droplets. Phys. Rev. Fluids 5, 083601. doi:10.1103/PhysRevFluids.5.083601.

[32] Thomson, S.J., Durey, M., Rosales, R.R., 2020b. Collective vibrations of a hydrodynamic active lattice. Proc. R. Soc. A 476, 20200155. doi:10.1098/rspa.2020.0155.

[33] Tinkham, M., 1996. Introduction to Superconductivity. McGraw-Hill, New York.

[34] Vachaspati, T., 2006. Kinks and domain walls: An introduction to classical and quantum solitons. Cambridge University Press, New York. doi:10.1017/CBO9780511535192.

A Appendix

A.1 Time-continuous dynamical model

We first wish to convert Eq. (1) from a discrete-time to a continuous-time dynamical system, under the assumption that $x_i(n+1) - x_i(n)$ and $v_i(n+1) - v_i(n)$ are "small." We follow this approach, which Meiss [22, p. 806] employs to turn the (discrete) standard map in the (continuous) equation of motion of a pendulum. Let us first modify the right-hand side of Eq. (1) so that v_i is not multiplied by C. Then, let us further restrict to the case of $M = 2$, which turns Eqs. (4) and (3) into the system

$$\begin{aligned}
\dot{v}_1(t) &= CK \sin\big(\omega v_1(t)\big) e^{-\nu v_1(t)^2} && \text{(6a)}\\
&\quad + K\eta\big(x_1(t) - x_2(t)\big) \operatorname{sgn}\big(x_1(t) - x_2(t)\big)\\
&\qquad \times e^{-\nu[x_1(t) - x_2(t)]^2},\\
\dot{x}_1(t) &= v_1(t), && \text{(6b)}\\
\dot{v}_2(t) &= CK \sin\big(\omega v_2(t)\big) e^{-\nu v_2(t)^2} && \text{(6c)}\\
&\quad + K\eta\big(x_2(t) - x_1(t)\big) \operatorname{sgn}\big(x_2(t) - x_1(t)\big)\\
&\qquad \times e^{-\nu[x_2(t) - x_1(t)]^2},\\
\dot{x}_2(t) &= v_2(t), && \text{(6d)}
\end{aligned}$$

where overdots denote derivatives with respect to t, and we henceforth leave the time dependence to be understood.

Now, without loss of generality assume that $x_1 < 0$ and $x_2 > 0$ during an interaction. The walkers cannot cross paths due to the repulsive mutual interaction. Hence, Eqs. (6) become

$$\begin{aligned}
\dot{v}_1 &= \hat{K} \sin\big(\omega v_1\big) e^{-\nu v_1^2} - KF\big(x_2 - x_1\big), && \text{(7a)}\\
\dot{x}_1 &= v_1, && \text{(7b)}\\
\dot{v}_2 &= \hat{K} \sin\big(\omega v_2\big) e^{-\nu v_2^2} + KF\big(x_2 - x_1\big), && \text{(7c)}\\
\dot{x}_2 &= v_2, && \text{(7d)}
\end{aligned}$$

having defined $\hat{K} := CK$ for convenience and the mutual interaction force as

$$F(\xi) = \eta(\xi) e^{-\nu \xi^2}. \tag{8}$$

Eliminating the v_i between Eqs. (7), we obtain

$$\begin{aligned}
\dot{x}_1 &= \hat{K} \sin\big(\omega \dot{x}_1\big) e^{-\nu \dot{x}_1^2} - KF\big(x_2 - x_1\big), && \text{(9a)}\\
\ddot{x}_2 &= \hat{K} \sin\big(\omega \dot{x}_2\big) e^{-\nu \dot{x}_2^2} + KF\big(x_2 - x_1\big). && \text{(9b)}
\end{aligned}$$

Equations (9) bear some similarity to those discussed in [14] (see also [13, 1]).

A.2 Weak-memory limit and effective Lagrangian

Note that the walker's self-interaction memory (i.e., the sine and exponentials on the left-hand sides of Eqs. (9)) depends on $v_i = \dot{x}_i$. Making a small slope approximation and neglecting higher-order terms, we obtain

$$\dot{x}_1 = \hat{\hat{K}}\dot{x}_1 - KF\big(x_2 - x_1\big), \tag{10a}$$

$$\ddot{x}_2 = \hat{\hat{K}}\dot{x}_2 + KF\big(x_2 - x_1\big). \tag{10b}$$

having defined $\hat{\hat{K}} := CK\omega$ for convenience.

Now, we observe that Eqs. (10) above are a system of Hamiltonian equations for the trajectories $\{x_i(t)\}$, derivable from the following *effective* Lagrangian density:

$$\mathcal{L}_{\text{eff}}[x_1(t), x_2(t)] = \frac{1}{2}\dot{x}_1^2 + \frac{\hat{\hat{K}}}{2}x_1^2 + \frac{1}{2}\dot{x}_2^2 + \frac{\hat{\hat{K}}}{2}x_2^2 - KU(x_2 - x_1), \tag{11}$$

by extremizing the action $\int \mathcal{L}_{\text{eff}}[x_1(t), x_2(t)]\,\mathrm{d}t$. In Eq. (11), $U(\xi)$ is the force potential such that $-U'(\xi) = F(\xi)$. Further, observe that Eq. (11) is also the Lagrangian of two nonlinearly coupled oscillators. The interaction force $F(\xi)$ is shown in Fig. 5. Clearly, the force is repulsive and monotone, which explains why walkers scatter (bounce) rather than annihilate or pass through each other. A more detailed analysis would be needed to reveal the multiple-bounce phenomena reported above.

Interestingly, due to the existence of a Lagrangian for the two-ODE description (10), this description of the interaction of two walkers can be thought of as a type of *collective coordinate* approximation [9] (see also [30, 8, 2, 19]). This analogy provides a framework for further analytical progress.

A.3 Calculating the fractal dimension

We calculate the Minkowski–Bouligand dimension by using the box-counting procedure. We use $0.2/2^{p-3}$ grid points, where $p = 9, 10, 11, 12$, for v_{in}. In each case v_{in} is partitioned into 2^j intervals of equal size, which corresponds to partitioning the square $(0, 0.2) \times (0, 0.2)$ into 2^j rectangles. Using $0.2/2^{p-3}$ points for each interval in the v_{in} direction, we sum up the number of intervals in the v_{out} direction of length $0.2/2^j$ that contains a v_{out} in each rectangle. This effectively partitions v_{out} into 2^j intervals, which then partitions the entire space into 2^{2j} squares (or boxes). We observe that for each case of $p = 9, \ldots, 12$, the Minkowski–Bouligand dimension given by (5) gives the same approximation, namely $d \approx 0.95$.

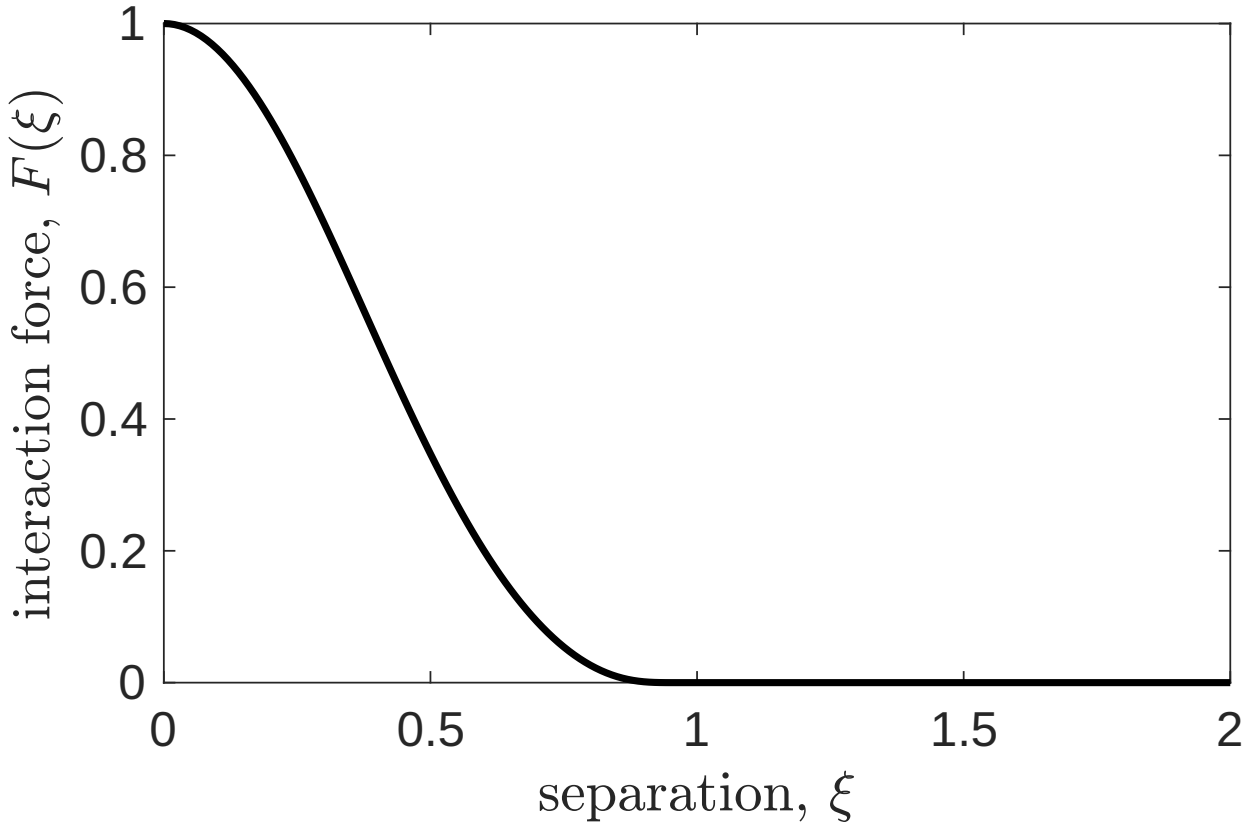

Figure 5: Interaction force between two walkers in the reduced time-continuous dynamical description, as a function of their separation $\xi = x_1 - x_2$, with $\omega = 15.5$ and $\nu \approx 2.8979$.